

Controlling arrival and service rates to reduce sensitivity of queueing systems with customer abandonment

Katsunobu Sasanuma^{*,a}, Robert Hampshire^b, Alan Scheller-Wolf^c

^aCollege of Business, Stony Brook University, Stony Brook, NY 11794, USA

^bFord School of Public Policy, University of Michigan, MI 48109, USA

^cTepper School of Business, Carnegie Mellon University, Pittsburgh PA 15213, USA

Abstract

The Erlang A model—an M/M/s queue with exponential abandonment—is often used to represent a service system with impatient customers. For this system, the popular square-root staffing rule determines the necessary staffing level to achieve the desirable QED (quality-and-efficiency-driven) service regime; however, the rule also implies that properties of large systems are highly sensitive to parameters. We reveal that the origin of this high sensitivity is due to the operation of large systems at a point of singularity in a phase diagram of service regimes. We can avoid this singularity by implementing a *congestion-based control* (CBC) scheme—a scheme that allows the system to change its arrival and service rates under congestion. We analyze a modified Erlang A model under the CBC scheme using a Markov chain decomposition method, derive non-asymptotic and asymptotic normal representations of performance indicators, and confirm that the CBC scheme makes large systems less sensitive than the original Erlang A model.

Key words: system with customer abandonment, Erlang A, reneging, balking, congestion-based control, sensitivity, phase diagram

*Corresponding author

Email addresses: katsunobu.sasanuma@stonybrook.edu (Katsunobu Sasanuma), hamp@umich.edu (Robert Hampshire), awolf@andrew.cmu.edu (Alan Scheller-Wolf)

1. Introduction

When a service facility is congested, we often observe impatient customers; they may decide to abandon the facility and leave, either by balking (not joining a queue) or reneging (leaving a queue). To evaluate the quality of service (QoS) of such facilities, it is convenient to use the Erlang A queueing model—an M/M/s queueing model with exponential reneging. The analysis of this model has revealed that three distinct asymptotic regimes exist: Quality-and-Efficiency-Driven (QED), Quality-Driven (QD), and Efficiency-Driven (ED) regimes [1, 2]. Among these regimes, QED is *practically* important since its delay probability (which we denote as P_Q) achieves a value strictly between 0 and 1, balancing good service and reasonable capacity cost. This QED regime is realized following the square-root staffing rule, i.e., setting the number of staff s in the vicinity of the square root of the resource requirement $R = \lambda/\mu$, where λ is an arrival rate and μ is a service rate per worker. For example, for a large system with $R = 10,000$, s could be set between $R \pm \sqrt{R} = 9,900 - 10,100$, which suggests that the control range of s is within $\pm 1\%$ of R . At the limit of large R , the control range of s , when normalized by R , approaches zero. Hence, a small fluctuation of s , λ , or μ , and thus s/R could make the system fall into either the ED ($P_Q \approx 1$) or QD ($P_Q \approx 0$) regimes. In fact, it has been pointed out that for large systems, “the above three-regime dichotomy is rather delicate” [2] and “operating in the QED regime, the performance measures tend to be highly sensitive to changes in the arrival rate, the service rate, or the number of servers” [3]. Thus, in order to maintain a system operating in a QED regime, facility operators need to constantly alter the staffing level in response to variations in the arrival and service rates; otherwise, the system could easily suffer from extreme delay probabilities—100% or 0%. Such a drastic fluctuation is obviously unfavorable for business. However, most previous literature focused on refining square-root staffing rules, and has not explained the origin of, or provided solutions to, this extreme sensitivity.

To reduce the sensitivity of the QoS for a system with customer abandon-

ment, we propose a *congestion-based-control* (CBC) scheme that controls the system's arrival and service rates during congestion. The implementation of the CBC scheme is commonly observed in practice: facility managers may try to temporarily suppress their arrival rate by informing customers a system is congested; they may also try to induce a faster service rate by providing staff with monetary incentives when a system is congested.

To evaluate the impact of the CBC scheme, we study a modified Erlang A model, in which the original Erlang A model is extended to incorporate either reneging or balking, and is allowed to change arrival and service rates during congestion. We provide both non-asymptotic and asymptotic normal representations of performance indicators for our modified Erlang A model. A non-asymptotic representation provides numerically accurate formulae to calculate performance indicators for even small systems, for which the asymptotic formulae are not reliable. An asymptotic representation provides insights into the sensitivity of the modified Erlang A system, i.e., operation at a point of singularity in a phase diagram, and explains a simple rule-of-thumb on how to avoid a singularity, expand the range of the *desired* QED regime, and achieve stable operations of large systems. Specifically, we show that under the CBC scheme, the square-root staffing rule to realize the QED regime is converted to the linear staffing rule, making the control range of the number of servers to maintain the QED regime the order of R instead of \sqrt{R} . Thus the system under the CBC scheme becomes more robust and less sensitive to parameters than the original Erlang A model.

The remainder of this paper is organized as follows. Section 2 reviews the related literature. Section 3 explains the modified Erlang A model with the CBC scheme. In Section 4, we take a Markov chain decomposition approach to represent performance indicators using blocking probabilities of decomposed sub-chains and obtain a non-asymptotic normal representation of performance indicators. In Section 5, we take a limit of large systems and derive phase diagrams of service regimes. We show the results of numerical experiments in Section 6. Finally, Section 7 concludes the paper.

2. Literature Review

Customer abandonment, such as reneging (leaving a queue while waiting) and balking (leaving a system before joining a queue), has been one of the main interests in queueing systems for a very long time. [4] built a multi-server queueing model with reneging, the Erlang A ($M/M/n+M$) model, that allows customers to abandon a system. In this system, each arrival has exponential patience and reneges if the waiting time exceeds the patience. [5, 6, 7] studied customer abandonment using a single server queueing model. They not only analyzed reneging, but also balking using the same framework and provided exact solutions [7]; however, their exact solutions are only numerically tractable.

In more recent years, researchers have been interested in obtaining intuition and simple rules-of-thumb that can be used by practitioners. For this purpose, they have developed various approximation techniques. One of the most frequently used methods is heavy-traffic approximation, which is sufficiently accurate when congestion is persistent. Researchers have found many simple rules-of-thumb for congested systems by applying heavy-traffic approximation. For example, heavy-traffic approximation has been applied to on-street parking problems [8], public housing applications [9], and kidney transplantations [10].

Heavy-traffic approximation is simple and effective, but it can only be applied to a system under heavy congestion. To study a system not in heavy congestion, [11] apply an asymptotic method (diffusion approximation) to analyze the Erlang C model (an $M/M/s$ queue with no customer abandonment) and provide an important, yet simple, square-root staffing rule to identify the staffing level that satisfies a desired QoS level. [1] apply the same asymptotic framework to the Erlang A model and classify its performance into three distinctive phases (regimes): QED (asymptotic limit of the probability of queueing P_Q is strictly between 0 and 1), QD ($P_Q \rightarrow 0$), and ED ($P_Q \rightarrow 1$).

The square-root staffing rule and its more refined variations have been well-studied [see, for example, 12, 13, 14, 15, 16, 17, 18, 19]. Although these analysis provide accurate results for the Erlang A and its generalized models, the facil-

ities represented by these models commonly exhibit a fundamental operational problem: high sensitivity of the QoS properties for systems with customer abandonment. The study conducted by [3] analyzed the sensitivity of performance indicators to changes in the model parameters, and concluded that “performance is quite sensitive to small percentage changes in the arrival rate or the service rate.” The fundamental problem is in the square-root staffing rule: the control range of the appropriate number of servers (staff members) to achieve the QED regime is of the order of \sqrt{R} , where $R = \lambda/\mu$. Thus, when systems are large (with large R), the control range (normalized by the system size) becomes very small. In fact, the QED regime that exists in between two extreme (QD and ED) regimes is rather delicate, as pointed out by [2]. Thus, when arrival and service rates fluctuate (as they often do in practice), the performance of the system could drastically change due to a slight change of R .

In practice, to prevent such fluctuations, operators often try to control the system by changing its characteristics over time. According to [20], four different control schemes can be considered as effective measures: (1) Control of the number of staff, (2) Control of the arrival rate, (3) Control of the service rate, and (4) Control of the queue discipline. Out of these four possible schemes, (1) and (4) have been analyzed in [21], but it is not always possible to quickly change staff or discipline especially when changes in parameters are unexpected. An alternative, more manageable approach could be (2) or (3). As an example of (2), [22] consider the trade-off between blocking arrivals and server idleness, leading to an optimal threshold queue admission policy. Another example is [23]: They study an admission control policy within a revenue maximization framework for large-scale systems that operate in the QED regime. Options (2) and (3) are often studied jointly; such examples include [24] and [25], whose objective is to minimize long-run average costs. These examples demonstrate the effectiveness of (2) and (3); however, most previous literature focuses on the long-run average cost, and does not attempt to explain how the measures of (2) and (3) could reduce the sensitivity of large-scale abandonment systems. In this paper, we consider (2) and (3)—controlling arrival and/or service rates

under congestion—and call these measures the *congestion-based control* (CBC) scheme. Our analysis reveals the root cause of the highly sensitive property of abandonment systems, enabling us to utilize the CBC scheme to make such systems more robust.

We study a modified Erlang A model with the CBC scheme, which considers two types of abandonment (reneging/balking). Our analysis employs the Markov chain decomposition approach: Following [26], we decompose the entire system into two sub-systems, an M/M/s/s queue and the reneging/balking queue, and analyze each sub-system separately. The same approach has been utilized to solve other variations of abandonment systems [27, 28]. This decomposition approach has three major analytical benefits. First, it reveals the relationship between the full system and the sub-systems to help us understand how each sub-system contributes to the system performance. Specifically, for this modified Erlang A model, when the two resource requirements (R for the M/M/s/s queue and R_Q for the reneging/balking queue) match, we observe a singularity point in which three regimes (QD, ED, and QED) co-exist in a phase diagram of asymptotic service regimes. Since this singularity is the root cause of the high sensitivity of the full system, we can make large systems more robust by simply making the two resource requirements of sub-systems different and eliminating the singularity; this simple idea is the primary insight into the CBC scheme. The second benefit is that the decomposition method makes the calculation procedure efficient by utilizing the previously known results for the M/M/s/s and the reneging/balking queues; for example, we can utilize the analytical results of sub-chains shown in [27] and [28]. Lastly, the decomposition approach makes the analysis easier since each decomposed sub-chain is elementary and its approximate analytical properties are simply described by Poisson/normal probability functions.

In summary, the contributions of this paper are: 1) we derive non-asymptotic and asymptotic representations for the QoS performance indicators of the modified Erlang A system following the Markov chain decomposition approach; 2) we reveal how the CBC scheme can avoid singularity in the phase diagram of

service regimes and make large systems more robust to changes in model parameters; and 3) we show that the CBC scheme converts the square-root staffing rule into the linear staffing rule in the asymptotic limit of large systems.

3. Modified Erlang A Model

3.1. Setup of the Model

Our modified Erlang A model is a simple extension of the original Erlang A model. Figure 1 shows the Markov chain (MC) structure of the modified Erlang A reneging model.

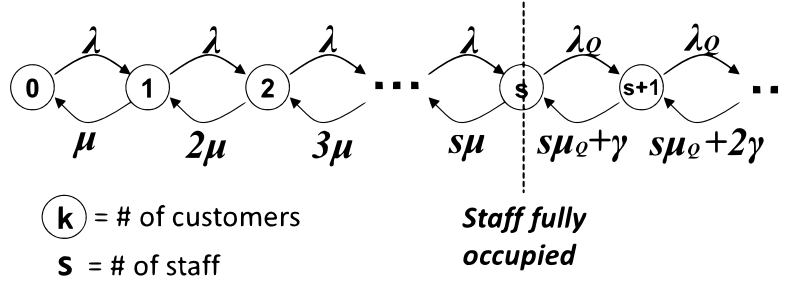


Figure 1: The modified Erlang A model with exponential reneging.

We assume that there are s staff members in the system, the arrival process is Poisson with rate λ , and the service time is exponential with rate μ . Unlike the original Erlang A reneging model, the modified Erlang A model allows a step change in the baseline arrival and service rates when a system is busy: The arrival rate can drop by a proportion ε (≥ 0), and the service rate can increase/decrease by a proportion τ , where ε and τ are altered by a congestion-based control (CBC) policy. The arrival and service rates when a system is busy are defined as $\lambda_Q \doteq (1 - \varepsilon) \lambda$ and $\mu_Q \doteq (1 + \tau) \mu$, respectively. Additionally, the modified Erlang A model allows customer abandonment either through exponential reneging or state-dependent balking, but not both in the same model. Specifically, for the modified Erlang A reneging model, we assume that each customer in queue reneges after an exponentially distributed time with rate γ (> 0) (note: the $\varepsilon = \tau = 0$ case corresponds to the original Erlang A model);

for the modified Erlang A balking model, we assume that the arrival rate drops by a linear balking rate $\delta (> 0)$ for each additional customer in queue. In sum, the birth and death coefficients for the modified Erlang A reneging and balking models are presented as follows. (Note that $(\cdot)^+$ denotes a positive part.)

1. For the reneging system, the total arrival rate and the total service rate at state k are $\lambda_k = \begin{cases} \lambda & 0 \leq k < s \\ \lambda_Q & s \leq k \end{cases}$ and $\mu_k = \begin{cases} k\mu & 1 \leq k \leq s \\ s\mu_Q + (k-s)\gamma & s < k \end{cases}$.
2. For the balking system, the total arrival rate and the total service rate at state k are $\lambda_k = \begin{cases} \lambda & 0 \leq k < s \\ (\lambda_Q - \delta \cdot (k-s))^+ & s \leq k \end{cases}$ and $\mu_k = \begin{cases} k\mu & 1 \leq k \leq s \\ s\mu_Q & s < k \end{cases}$.

We define two resource requirements for the system: $R \doteq \lambda/\mu$ when a system is not busy and $R_Q \doteq \lambda_Q/\mu_Q$ when a system is busy. Since we implement the CBC policy to improve the performance of the system when it is busy, we only consider the case where both $R_Q \leq R$ and $\lambda_Q \leq \lambda$ hold; thus proportions ε and τ satisfy $0 \leq \varepsilon \leq 1$, $-1 \leq \tau \leq 1$, and $\varepsilon + \tau \geq 0$. (Note that we can use the same technique to discuss the cases $R_Q > R$ (a system slows down when it is busy) and/or $\lambda_Q > \lambda$ (more customers are attracted to join when a system is busy), but we do not discuss these cases in this paper.) Finally, we assume an independence among parameters: γ , δ , ε , and τ do not depend on λ , μ , s , or state k .

3.2. Decomposition of the Markov Chain

To solve the modified Erlang A model, we split the entire system into two sub-systems and analyze them separately since the two sub-systems, one when it is busy and the other when it is not, possess very different queueing properties, which are easy to analyze independently but complicated to study jointly. Specifically, we divide the full MC that represents the modified Erlang A model into an M/M/s/s sub-chain and a reneging/balking sub-chain, which overlap at state s . We denote the left sub-chain (M/M/s/s sub-system comprised of states 1 to s) as sub-chain 1, and the right sub-chain (reneging/balking sub-system comprised of states s or larger) as sub-chain 2. Customers are put in queue if

they enter when the system is in sub-chain 2. We denote the probabilities of being in sub-chains 1 and 2 as P_1 and P_2 , respectively. We denote the queueing probability (delay probability) as $P_Q (= P_2)$; the abandonment probability (abandonment includes both reneging and balking) as P_{ab} ; the expected number of customers in queue as L_Q ; and the expected time in queue as W_Q . All of these performance indicators can be represented using the steady-state probabilities of state s in the sub-chains and full MC, which are denoted as π_s^1 , π_s^2 , and π_s , respectively. For simplicity, we call π_s^1 , π_s^2 , and π_s the *blocking* probabilities of sub-chains 1, 2, and the full MC, respectively.

For analytical convenience, we introduce three parameters: (1) $p \doteq 1 - s\mu_Q/\lambda$, (2) $a = a_{s;R} \doteq (s - R)/R$, and (3) $c = c_{s;R} \doteq (s - R)/\sqrt{R}$. First, p represents a heavy-traffic limit of the abandonment probability¹ when $p > 0$ ($\lambda > s\mu_Q$), but p can also take a negative value depending on parameters. Second, a is a linear (staffing) coefficient of the number of staff s measured relative to R , in units of R . Finally, c is a square-root (staffing) coefficient of s measured relative to R , in units of \sqrt{R} . Note that from the non-negativity requirement on the number of staff s , $p \leq 1$, $a \geq -1$, and $c \geq -\sqrt{R}$ must be satisfied.

3.3. Quality-of-Service Performance Indicators

For the modified Erlang A model, the steady-state probability π_s as well as the QoS performance indicators such as the delay probability P_Q , the abandonment probability P_{ab} , and the average queue length L_Q can all be represented by the blocking probabilities of the sub-chains, π_s^1 and π_s^2 , as summarized in Lemma 1. We call these representations *structural* since they reveal how performance indicators are constructed from sub-chains. Note that we obtain the

¹Regardless of how a customer abandons a system, in a heavy-traffic limit, the system accommodates $s\mu_Q$ customers per unit time on average. Hence, the number of customers abandoning a system is $\lambda - s\mu_Q$, from which we obtain the heavy-traffic limit of P_{ab} as $(\lambda - s\mu_Q)/\lambda = 1 - \mu_Q/\lambda$.

performance indicators for the original Erlang A model as a special case by setting $\varepsilon = \tau = 0$ and $\theta = \gamma$ in Lemma 1. All proofs are in the Appendix.

Lemma 1. *Performance indicators of the modified Erlang A model are represented as follows:*

$$\frac{1}{\pi_s} = \frac{1}{\pi_s^1} + \frac{1}{\pi_s^2} - 1, \quad (1)$$

$$P_Q = \frac{\pi_s}{\pi_s^2} = \frac{\frac{1}{\pi_s^2}}{\frac{1}{\pi_s^1} + \frac{1}{\pi_s^2} - 1}, \quad (2)$$

$$P_{ab} = \frac{1 + p \cdot (\frac{1}{\pi_s^2} - 1)}{\frac{1}{\pi_s^2}} P_Q \quad (3)$$

$$= \frac{1 + p \cdot (\frac{1}{\pi_s^2} - 1)}{\frac{1}{\pi_s^1} + \frac{1}{\pi_s^2} - 1}, \quad (4)$$

$$L_Q = \frac{\lambda}{\theta} \cdot (P_{ab} - \varepsilon P_Q) \quad (5)$$

$$= \frac{\lambda}{\theta} \cdot \frac{(1 - \varepsilon) + (p - \varepsilon)(\frac{1}{\pi_s^2} - 1)}{\frac{1}{\pi_s^1} + \frac{1}{\pi_s^2} - 1}, \quad (6)$$

where

$$p = 1 - \frac{s\mu_Q}{\lambda} = 1 - (1 + \tau)(a + 1) = -(1 + \tau)a - \tau \quad (7)$$

and $\theta = \gamma$ (or δ) for a reneging (or balking) system.

Among the performance indicators presented in Lemma 1, we are most interested in the delay probability P_Q and the abandonment probability P_{ab} because a reduction of P_Q yields higher quality of a service system, and a reduction of P_{ab} leads to higher system throughput (i.e., the average number of customers being serviced per unit time: $X = \lambda \cdot (1 - P_{ab})$) and thus higher efficiency of the system. However, it may not be possible to achieve a reduction of P_Q and P_{ab} at the same time. To determine if a simultaneous reduction is possible, we can use the following exact relationship, which holds for any modified Erlang A model including the original Erlang A model. In this corollary, we denote π_s^1 as P_{block} .

Corollary 1. P_Q and P_{ab} for the modified Erlang A model satisfy the following equation:

$$P_{ab} = \frac{(p - P_{block}) P_Q + (1 - p) P_{block}}{1 - P_{block}}. \quad (8)$$

From Corollary 1, we can determine how P_Q and P_{ab} are dependent on abandonment-related parameters, such as γ (or δ) and ε :

Corollary 2. P_Q and P_{ab} for the modified Erlang A model satisfy the following properties:

1. P_Q is a monotonically decreasing function of abandonment-related parameters.
2. P_{ab} is a monotonically increasing (decreasing) function of abandonment-related parameters if $p < P_{block}$ ($p > P_{block}$, respectively). P_{ab} is independent of all abandonment-related parameters if $p = P_{block}$.

Corollary 2 says that if $p < P_{block}$, a trade-off exists and we need to control the level of abandonment in order to achieve an optimal balance between P_Q and P_{ab} . In contrast, if $p > P_{block}$, both P_Q and P_{ab} can be minimized simultaneously by controlling the level of abandonment. The best practice in such a case would be to block all arrivals when all staff members are busy. This case could occur when customers in queue significantly slow down the service speed of the system (or in other words, when waiting customers bring large negative externalities to the system). A similar phenomenon can be observed in a congested traffic network [29].

We can derive an alternative expression (corollary) to Lemma 1 using the stationary probability P_{Q-} of the system having customers in queue (i.e., the probability that the total number of customers in the system is greater than s):

$$P_{Q-} \doteq P_Q - \pi_s = \frac{\frac{1}{\pi_s^2} - 1}{\frac{1}{\pi_s^1} + \frac{1}{\pi_s^2} - 1}.$$

Corollary 3. *Performance indicators for the modified Erlang A model are also represented as follows:*

$$P_Q = \pi_s + P_{Q-}, \quad (9)$$

$$P_{ab} = \pi_s + p \cdot P_{Q-}, \quad (10)$$

$$L_Q = \frac{\lambda}{\theta} \cdot ((1 - \varepsilon)\pi_s + (p - \varepsilon)P_{Q-}). \quad (11)$$

Remark 1. *Both Corollary 3 and Lemma 1 are exact and general. From Corollary 3 we can derive various formulae and approximations, such as performance indicators for the Erlang B and C models, and heavy-traffic approximation. See the Appendix for more discussion.*

4. Non-asymptotic Poisson-Normal Approximation

In this section we derive a convenient non-asymptotic representation for performance indicators. We start by expressing all blocking probabilities of sub-chains using a Poisson representation; these probabilities are then converted into a normal representation. Finally, we aggregate blocking probabilities to obtain a non-asymptotic normal representation for the performance indicators of the full system.

4.1. Poisson Representation of Blocking Probabilities

The left sub-chain (an M/M/s/s queue) is a truncated M/M/ ∞ queue, whose steady-state probabilities are proportional to a Poisson distribution. Using this property, the blocking probability of the left sub-chain, known as the Erlang B (or Erlang Loss) formula, can be represented as a function of a Poisson CDF and PMF with rate parameter R and index s . This index s is implicitly assumed to be an integer because it corresponds to the staffing level. Similarly, the right sub-chain can also be regarded as a truncated M/M/ ∞ queue if we rescale the rate parameter and index, where again the rescaled index is assumed to be an integer. Under this integer constraint, the blocking probability of the right sub-chain can also be represented as a function of a Poisson CDF and PMF. Note

Table 1: PMF/PDF/CDF of R.V.'s

	Poisson R.V. with mean R	Normal R.V. with mean R and standard deviation \sqrt{R}	Standard Normal R.V.
R.V.	$X_P \sim \text{Pois}(R)$	$X_N \sim N(R, R)$	$Z \sim N(0, 1)$
CDF	$F_P(\cdot; R)$	$F_N(\cdot; R, R)$	$\Phi(\cdot)$
PMF/PDF	$f_P(\cdot; R)$	$f_N(\cdot; R, R)$	$\phi(\cdot)$

that the integer constraints for the staffing level (left sub-chain) and the rescaled staffing level (right sub-chain) are both dropped when we convert the Poisson representation to a normal representation, while the continuity correction terms need to be added to the normal representation in order to account for the inevitable error associated with this discrete-to-continuous Poisson to normal conversion.

To prepare for the derivation, we define new R.V.'s and functions in Table 1: Poisson, normal, and standard normal R.V.'s and associated probability mass function (PMF), probability density function (PDF), and cumulative distribution function (CDF). We introduce three Poisson R.V.'s: X_P for the left sub-chain, X'_P and X''_P for the reneging and balking models' right sub-chains, respectively. The distribution of each Poisson R.V. is represented by its rate parameter and staffing level. Using the notation in Table 2 and assuming non-negative integral staffing levels, we are able to obtain a Poisson representation for all blocking probabilities:

Lemma 2. *For any (possibly rescaled) positive rate parameters (R, R', R'') and non-negative integral staffing levels (s, s', s'') , inverse blocking probabilities for the left sub-chain (sub-chain 1) and the right sub-chain (sub-chain 2) are exactly represented as follows:*

1. $M/M/s/s$ sub-chain (left sub-chain):

$$\frac{1}{\pi_s^1} = \frac{F_P(s; R)}{f_P(s; R)}, \quad (12)$$

Table 2: Setup for Poisson representation

Sub-chain	Poisson R.V.	Rate Parameter	Staffing level
M/M/s/s	$X_P \sim \text{Pois}(R)$	$R \doteq \frac{\lambda}{\mu}$	s
Reneging	$X'_P \sim \text{Pois}(R')$	$R' \doteq \frac{\lambda_Q}{\gamma} = (1 - \varepsilon)(\mu/\gamma)R$	$s' \doteq \frac{s\mu_Q}{\gamma} = \frac{\mu_Q}{\gamma} \cdot s$
Balking	$X''_P \sim \text{Pois}(R'')$	$R'' \doteq \frac{s\mu_Q}{\delta} = \frac{(a+1)\mu_Q}{\delta} \cdot R$	$s'' \doteq \frac{\lambda_Q}{\delta} = \frac{1 - \varepsilon}{1 + \tau} \cdot \frac{\mu_Q}{(a+1)\delta} \cdot s$

Note: $\lambda_Q \doteq (1 - \varepsilon)\lambda$ and $\mu_Q \doteq (1 + \tau)\mu$. From $a \doteq (s - R)/R$, $s = (a + 1)R$ holds.

2. *Reneging sub-chain (right sub-chain):*

$$\frac{1}{\pi_s^2} = 1 + \frac{1 - F_P(s' : R')}{f_P(s' : R')}, \quad (13)$$

3. *Balking sub-chain (alternate right sub-chain):*

$$\frac{1}{\pi_s^2} = \frac{F_P(s'' : R'')}{f_P(s'' : R'')}. \quad (14)$$

To convert these Poisson representations to normal, we need to find the relationship between the Poisson CDF/PMF and the normal CDF/PDF, which is discussed next.

4.2. Normal Representation of Blocking Probabilities

A Poisson distribution is well approximated by the normal distribution with the same mean and standard deviation as long as the mean (rate parameter) of the Poisson is sufficiently large. This approximation is based on the Central Limit Theorem. Using this property, we can convert the Poisson CDF/PMF to the normal CDF/PDF, and ultimately to the standard normal CDF/PDF.

For convenience, we call $f_P(s; R)/(1 - F_P(s; R))$ the “modified” hazard function of the Poisson distribution² and $h(x) \doteq \phi(x)/(1 - \Phi(x)) (= \phi(-x)/\Phi(-x))$ the hazard function of the standard normal distribution. We represent the conversion formulae in two different ways: using R and c and also using a and c .

²We use the term “modified” because the hazard function for a discrete R.V. is usually defined slightly differently as $\Pr(X_P = s)/(1 - \Pr(X_P \leq s - 1))$. See [30].

The former is suitable when making a non-asymptotic analysis (a finite R case) and the latter is suitable when making an asymptotic analysis (an infinite R case).

Proposition 1. *For a sufficiently large R and a non-negative integer s , the Poisson distribution with mean (rate parameter) R and index s and the “modified” hazard function of the Poisson distribution are well-approximated by the standard normal:*

$$F_P(s; R) \approx \Phi(c_{s;R} + \Delta_R), \quad (15)$$

$$f_P(s; R) \approx \frac{\phi(c_{s;R} + \Delta_R)}{\sqrt{R}} = \frac{a_{s;R} \cdot \phi(c_{s;R} + \Delta_R)}{c_{s;R}}, \quad (16)$$

$$\frac{f_P(s; R)}{1 - F_P(s; R)} \approx \frac{h(c_{s;R} + \Delta_R)}{\sqrt{R}} = \frac{a_{s;R} \cdot h(c_{s;R} + \Delta_R)}{c_{s;R}}, \quad (17)$$

and

$$\frac{f_P(s; R)}{F_P(s; R)} \approx \frac{h(-c_{s;R} - \Delta_R)}{\sqrt{R}} = \frac{a_{s;R} \cdot h(-c_{s;R} - \Delta_R)}{c_{s;R}}. \quad (18)$$

Observe in Proposition 1 that while the Poisson representation requires s to be a non-negative integer, the normal representation does not. However, to account for the errors caused by the Poisson-to-normal (discrete-to-continuous) conversion, a continuity correction term Δ_R appears in the normal representation. This correction term Δ_R is non-negligible when R is small (for example, if R is around 10), but diminishes to zero if R is large. Note that Proposition 1 without the Δ_R term is equivalent to the Poisson-to-normal conversion formulae seen in several textbooks (for example, see [31] and [32]). However, we are interested in both small and large R , so we maintain Δ_R in our formulae.

Remark 2. *Proposition 1 relies on the Central Limit Theorem that is applied to the sum, R , of i.i.d. Poisson R.V.’s with mean 1. Thus, if R is very small, the approximation becomes imprecise. If we need more accurate results for a smaller R case, we can use the Wilson-Hilferty approximation [33, 34]. According to this approximation, we can convert the Poisson CDF and PMF as*

Table 3: Notation for standard normal representation

Sub-chain	Standard Normal R.V.	Square-root Coef	Linear Coef	Continuity Correction
M/M/s/s	$Z \sim N(0, 1)$	$c \doteq c_{s;R}$	$a \doteq a_{s;R}$	$\Delta \doteq \Delta_R$
Reneging	$Z' \sim N(0, 1)$	$c' \doteq c_{s';R'}$	$a' \doteq a_{s';R'}$	$\Delta' \doteq \Delta_{R'}$
Balking	$Z'' \sim N(0, 1)$	$c'' \doteq c_{s'';R''}$	$a'' \doteq a_{s'';R''}$	$\Delta'' \doteq \Delta_{R''}$

Note: $a_{s;R} \doteq (s - R)/R$, $c_{s;R} \doteq (s - R)/\sqrt{R}$, $\Delta_R \doteq 0.5/\sqrt{R}$.

follows: $F_P(s; R) \approx \Phi(z(s, R))$, $f_P(s; R) \approx \Phi(z(s, R)) - \Phi(z(s - 1, R))$, where $z(s, R) \doteq \frac{\sqrt[3]{\frac{R}{s+1} - 1 + \frac{1}{9(s+1)}}}{\frac{1}{3\sqrt{s+1}}}$. While this approximation does not support an asymptotic analysis, it is very accurate even for $R = 1$ and easy to calculate using a spreadsheet. Hence, the non-asymptotic formulae based on the Wilson-Hilferty approximation provide an important alternative to the non-asymptotic formulae that are based on the Central Limit Theorem for systems with very small means.

We are now ready to derive the blocking probabilities in a standard normal representation. By combining Lemma 2 and Proposition 1 with the notation defined in Table 3, we obtain the following lemma. (Note that in this lemma, all integer constraints have been dropped.)

Lemma 3. *For sufficiently large (at least around 10) rate parameters (R , R' , R''), inverse blocking probabilities of sub-chains are approximated by the hazard function for the standard normal distribution as follows:*

1. *M/M/s/s sub-chain (left sub-chain):*

$$\frac{1}{\pi_s^1} \approx \frac{\sqrt{R}}{h(-c - \Delta)} \text{ or } \frac{1}{a \cdot h(-c - \Delta)/c}, \quad (19)$$

2. *Reneging sub-chain (right sub-chain):*

$$\frac{1}{\pi_s^2} \approx 1 + \frac{\sqrt{R'}}{h(c' + \Delta')} \text{ or } 1 + \frac{1}{a' \cdot h(c' + \Delta')/c'}, \quad (20)$$

3. *Balking sub-chain (alternate right sub-chain):*

$$\frac{1}{\pi_s^2} \approx \frac{\sqrt{R''}}{h(-c'' - \Delta'')} \text{ or } \frac{1}{a'' \cdot h(-c'' - \Delta'')/c''}. \quad (21)$$

Table 4: Parameters characterizing normal representation

Sub-chain	Square-root Coefficient	Linear Coefficient	Rate Parameter
M/M/s/s	$c (= a\sqrt{R})$	$a (= c/\sqrt{R})$	$R (= (c/a)^2)$
Reneging	$c' = \frac{a_Q}{a} \sqrt{\frac{1+\tau}{1-\varepsilon}} \sqrt{\frac{\mu_Q}{\gamma}} \cdot c$	$a' = \frac{1+\tau}{1-\varepsilon} \cdot a_Q$	$R' = \frac{1-\varepsilon}{1+\tau} \cdot \frac{\mu_Q}{\gamma} R = \frac{(1-\varepsilon)\mu}{\gamma} R$
Balking	$c'' = -\frac{a_Q}{a} \sqrt{\frac{\mu_Q}{(a+1)\delta}} \cdot c$	$a'' = -\frac{a_Q}{a+1}$	$R'' = \frac{(a+1)\mu_Q}{\delta} R$

Note: $a_Q = a$ and $(1+\tau)/(1-\varepsilon) = 1$ hold if $\varepsilon + \tau = 0$ (i.e., $R = R_Q$).

Table 5: Non-asymptotic normal representation of the Modified Erlang A model

Performance Indicator	Reneging system	Balking system
π_s	$\frac{1}{\sqrt{R}} \cdot \frac{1}{\frac{1}{h(-c-\Delta)} + \frac{\sqrt{(1-\varepsilon)\mu/\gamma}}{h(c'+\Delta')}}}$	$\frac{1}{\sqrt{R}} \cdot \frac{1}{\frac{1}{h(-c-\Delta)} + \frac{\sqrt{(a+1)\mu_Q/\delta}}{h(-c''-\Delta'')} - \frac{1}{\sqrt{R}}}}$
P_{Q-}	$\frac{\frac{\sqrt{(1-\varepsilon)\mu/\gamma}}{h(c'+\Delta')}}{\frac{1}{h(-c-\Delta)} + \frac{\sqrt{(1-\varepsilon)\mu/\gamma}}{h(c'+\Delta')}}}$	$\frac{\frac{\sqrt{(a+1)\mu_Q/\delta}}{h(-c''-\Delta'')} - \frac{1}{\sqrt{R}}}{\frac{1}{h(-c-\Delta)} + \frac{\sqrt{(a+1)\mu_Q/\delta}}{h(-c''-\Delta'')} - \frac{1}{\sqrt{R}}}}$

4.3. Non-asymptotic Normal Representation of Performance Indicators

We derive the non-asymptotic normal representation and corresponding staffing rule for the modified Erlang A model. For this purpose, we first find the relationships among key parameters of sub-chains: square-root coefficients, linear coefficients, and rate parameters. To simplify expressions, we introduce a parameter $a_Q \doteq \frac{s-R_Q}{R} = a + \frac{R-R_Q}{R} = a + \frac{\varepsilon+\tau}{1+\tau}$. Using Tables 2 and 3, we obtain Table 4. Combining Lemma 1 and Lemma 3 with the help of Table 4, we can derive the non-asymptotic normal representation of π_s and P_{Q-} as shown in Table 5. P_Q and P_{ab} are obtained from these π_s and P_{Q-} using Corollary 3. Note that these non-asymptotic formulae cannot be represented by a single parameter c or a in contrast to the case for the popular Erlang A square-root staffing rule since the non-asymptotic formulae depend on the size of the system (thus, requiring any two of the three parameters: a , c , and $R (= (c/a)^2)$).

The decision rule for the optimal number of staff that satisfies a specific QoS target is obtained as a direct application of the non-asymptotic normal representation of performance indicators:

Proposition 2. *Assume that a specific QoS requirement is either $P_Q < \alpha$ (< 1) or $P_{ab} < \alpha$ (< 1), where the forms of P_Q and P_{ab} are specified as $P_Q = \pi_s + P_{Q-}$ and $P_{ab} = \pi_s + p \cdot P_{Q-}$ using π_s and P_{Q-} in Table 5. Then, given R , the minimum number of staff $s_{\alpha;R}$ that is required to guarantee the QoS requirement is obtained as $s_{\alpha;R} = \lceil R + c_{\alpha;R}\sqrt{R} \rceil$ ($s_{\alpha;R} = \lceil R + a_{\alpha;R}R \rceil$), where $c_{\alpha;R}$ ($a_{\alpha;R}$, respectively) is the unique solution to either $P_Q = \alpha$ or $P_{ab} = \alpha$.*

5. Asymptotic Normal Approximation

In this section we derive analytical expressions for the asymptotic properties of the modified Erlang A model in each regime (i.e., QD, QED, or ED) and obtain phase diagrams of service regimes in the asymptotic limit. We see that under CBC, the modified Erlang A model has a wider QED regime than the original Erlang A model; this wider QED regime is described by a linear staffing rule (parameterized by a) as opposed to the square-root staffing rule (parameterized by c) of the original Erlang A model.

5.1. Asymptotic Normal Representation of Performance Indicators

Before we start the derivation, recall that in Lemma 1, performance indicators are represented by inverse blocking probabilities of sub-chains. We thus need to find the asymptotic limit of each blocking probability on an appropriate scale. Notice that each sub-chain exhibits its congestion property—either saturated or idling—depending on whether the staffing level (number of servers or staff members) is below or above the sub-chain’s scale parameter, respectively. Since each sub-chain is indexed by its own scale parameter (R for the left sub-chain and R_Q for the right sub-chain), under the assumption $R_Q \leq R$, we can identify that, in the asymptotic limit of large systems, the modified Erlang A model as a whole should exhibit a QD regime when we maintain $s < R_Q$ (both

sub-systems are mostly idling) or an ED regime when we maintain $R < s$ (both sub-systems are mostly saturated). The most interesting case, leading to the QED regime, is when (1) $R_Q < s < R$ (under the condition that $R_Q < R$ or equivalently, $\varepsilon + \tau > 0$), in which the left sub-chain is mostly saturated while the right sub-chain is mostly idling, or (2) $s \approx R = R_Q$ (under the condition that $R_Q = R$ or equivalently, $\varepsilon + \tau = 0$), in which both sub-chains are neither idling nor saturated.

For the first ($R_Q < s < R$) case, since there is a wider region in which s achieve the QED regime, we utilize a linear staffing representation and express blocking probabilities using a linear coefficient a ; see Table 6 for the analytical results of inverse blocking probabilities on a linear scale. For the second ($s \approx R = R_Q$) case, to explain the congestion properties of large systems, we utilize a finer, square-root staffing representation, and express blocking probabilities using a square-root coefficient c ; see Table 7 for the analytical results of inverse blocking probabilities on a square-root scale.

By plugging the inverse blocking probabilities in Tables 6 and 7 into Equations (2) and (4) in Lemma 1, the asymptotic representation of performance indicators for the modified Erlang A model is derived in Table 8. Note that $\phi(c)$ in Table 8 is defined as

$$\phi(c) \doteq \frac{\frac{\sqrt{\mu_Q/\theta}}{h(\sqrt{\mu_Q/\theta \cdot c})}}{\frac{1}{h(-c)} + \frac{\sqrt{\mu_Q/\theta}}{h(\sqrt{\mu_Q/\theta \cdot c})}}, \quad (22)$$

where $\theta = \gamma$ (or δ) for a reneging (or balking) system.

To summarize this subsection, in the QED regime, we obtain a square-root staffing rule when both sub-chains change their congestion properties at the same threshold $s \approx R = R_Q$, while we obtain a linear staffing rule when the left sub-chain is mostly saturated and the right sub-chain is mostly idling when $R_Q < s < R$.

Remark 3. *The process to derive asymptotic formulae shows two important distinctions between small systems and large systems. First, π_s in Corollary 3*

Table 6: Asymptotic limit of blocking probabilities on a linear scale when $R_Q < R$

sub-chain	$0 \leq s < R_Q$	$R_Q < s < R$	$R < s$
M/M/s/s	$a < 0, c \rightarrow -\infty, \frac{1}{\pi_s^1} \rightarrow -\frac{1}{a}$	same as the left	$a > 0, c \rightarrow +\infty, \frac{1}{\pi_s^1} \rightarrow +\infty$
Reneging	$a' < 0, c' \rightarrow -\infty, \frac{1}{\pi_s^2} \rightarrow +\infty$	same as the right	$a' > 0, c' \rightarrow +\infty, \frac{1}{\pi_s^2} \rightarrow \frac{a+1}{a_Q}$
Balking	$a'' > 0, c'' \rightarrow +\infty, \frac{1}{\pi_s^2} \rightarrow +\infty$	same as the right	$a'' < 0, c'' \rightarrow -\infty, \frac{1}{\pi_s^2} \rightarrow \frac{a+1}{a_Q}$

 Table 7: Asymptotic limit of blocking probabilities on a square-root scale when $R = R_Q$

sub-chain	$0 \leq s < R_Q$	$s \approx R = R_Q$ ($s = R + c\sqrt{R}$)	$R < s$
M/M/s/s	*	$c, a \rightarrow 0, \frac{1}{\pi_s^1} \rightarrow +\infty, \frac{a}{\pi_s^1} \rightarrow \frac{1}{h(-c)/c}$	*
Reneging	*	$c' = \sqrt{\frac{\mu_Q}{\gamma}} \cdot c, a' \rightarrow 0, \frac{1}{\pi_s^2} \rightarrow +\infty, \frac{a}{\pi_s^2} \rightarrow \frac{1}{h(c')/c'}$	*
Balking	*	$c'' \rightarrow -\sqrt{\frac{\mu_Q}{\delta}} \cdot c, a'' \rightarrow 0, \frac{1}{\pi_s^2} \rightarrow +\infty, \frac{a}{\pi_s^2} \rightarrow -\frac{1}{h(-c'')/c''}$	*

Note: The symbol * indicates the same convergence properties as Table 6 except that $a_Q = a$ holds in this table (Table 7), where $R = R_Q$ (i.e., $\varepsilon + \tau = 0$ and thus $a_Q = a$) is assumed.

Table 8: Asymptotic representation of the modified Erlang A

	ED Regime	QED Regime		QD Regime
Perf	$0 \leq s < R_Q$	$R_Q < s < R$	$s \approx R$ ($s = R + c\sqrt{R}$)	$R < s$
Ind		(when $R_Q < R$)	(when $R_Q = R$)	
P_Q	1	$\frac{1}{1 - \frac{a_Q}{a}} = \frac{1 - \frac{s}{R}}{1 - \frac{R_Q}{R}}$	$\phi(c)$	0
P_{ab}	p	$\frac{\varepsilon}{1 - \frac{a_Q}{a}} = \frac{\varepsilon \left(1 - \frac{s}{R}\right)}{1 - \frac{R_Q}{R}}$	$\varepsilon \phi(c)$	0

Notes: $p \doteq 1 - (1 + \tau)(a + 1)$, $a_Q \doteq \frac{s - R_Q}{R} = a + \frac{\varepsilon + \tau}{1 + \tau}$.

(non-asymptotic representation) is dropped in Table 8 (asymptotic representation) because π_s in Table 5 approaches zero as R increases. Second, all continuity correction terms in Table 5 become negligible as R increases. These observations imply that inaccuracies for asymptotic formulae are due to the discrete state space of Markov chains. For small systems, the discreteness of the state space of Markov chain impacts the values of performance indicators, while for large systems we can ignore the contribution from any single state since its contribution is negligible when systems are large. We examine the difference between non-asymptotic and asymptotic formulae using numerical experiments in Section 6.

Remark 4. Although the modified Erlang A reneging and balking models have different non-asymptotic representations as shown in Table 5, their asymptotic representations exactly match in Table 8. This result implies that both (exponential) reneging and (linear) balking asymptotically contribute to delay and abandonment probabilities in the same way, although they are often discussed in different contexts. This coincidence is intuitively explained as follows: If the size of a system increases, the discreteness a system exhibits becomes smaller, continuity correction terms diminish, π_s diminishes, and the time intervals between reneging (or balking) diminish. In this case, given $\gamma = \delta$, there is no difference in the impact of reneging and balking to the QoS properties (P_Q and P_{ab}) of the system because customers constantly exit from the system with the same rate proportional to the size of the queue (i.e., a fluid approximation applies). However, note that the delay (W_Q) is different between reneging and balking systems; a balking system has a lower W_Q because fewer customers join the system than a reneging system.

5.2. Phase Diagram

To understand the congestion properties of the modified Erlang A model in the asymptotic limit of large systems, it is convenient to observe the phase diagram of the three service regimes. In this phase diagram we do not distinguish

between reneging and balking models since they share the same asymptotic results. We use an index $1 - \frac{R_Q}{R}$ to represent the level of intervention, which ranges from 0 (no intervention case when $\frac{R_Q}{R} = \frac{1-\varepsilon}{1+\tau} = 1$) to 1 (full intervention case when $R_Q = 1 - \varepsilon = 0$). The “no intervention” case corresponds to the CBC scheme with $\varepsilon + \tau = 0$, which includes the original Erlang A model ($\varepsilon = \tau = 0$) as a special case. The “full intervention” case corresponds to the CBC scheme with $\varepsilon = 1$ (customers’ arrivals are blocked when all servers are full), which makes the modified Erlang A model equivalent to the Erlang B model. The phase boundaries of asymptotic service regimes in these diagrams are $s = R$ and $s = R_Q (= \frac{1-\varepsilon}{1+\tau}R \leq R)$ since the modified Erlang A model contains two sub-systems indexed by resource requirements R and R_Q . Thus, for a given level of intervention $1 - \frac{R_Q}{R}$, a system achieves QED in the asymptotic limit when the staffing level (measured in R) is $\frac{R_Q}{R} (= \frac{1-\varepsilon}{1+\tau}) < \frac{s}{R} < \frac{R}{R} (= 1)$ (see Figure 2), or equivalently, when the traffic intensity is $\frac{R}{R} (= 1) < \frac{R}{s} < \frac{R}{R_Q} (= \frac{1+\tau}{1-\varepsilon})$ (see Figure 3). For simplicity of presentation, we denote the modified Erlang A with $\varepsilon + \tau = 0$ ($R = R_Q$) as the Erlang Ae in Figures 2 and 3. Erlang A ($\varepsilon = \tau = 0$) is a special case of Erlang Ae in this case.

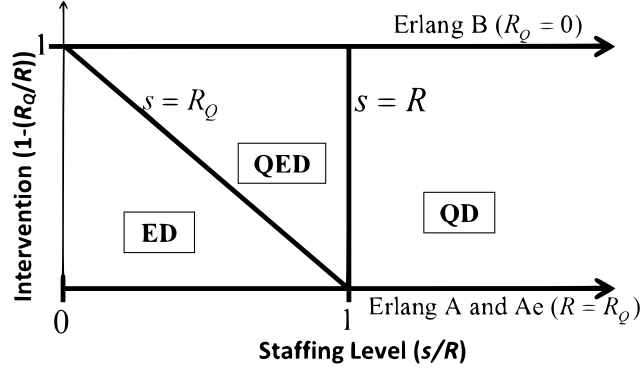


Figure 2: Phase diagram (staffing level representation) for the modified Erlang A model.

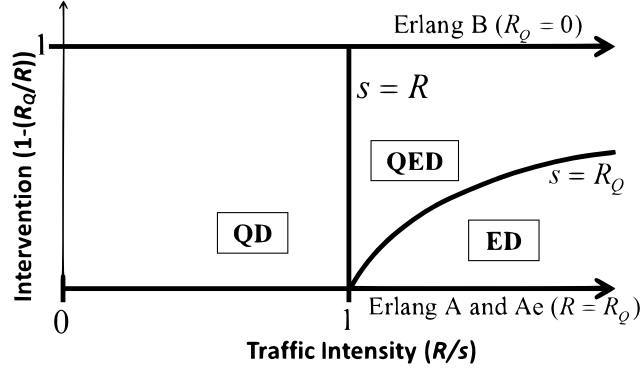


Figure 3: Phase diagram (traffic intensity representation) for the modified Erlang A model.

These phase diagrams not only reveal asymptotic service regimes according to a given staffing level and intervention, but also provide visual information about robustness (i.e., sensitivities to changes in parameters). Specifically, we observe in Figures 2 and 3 that $s = R$ when $R = R_Q$ (no intervention case; the bottom edge of the phase diagram) is a singular point, where all three regimes co-exist at a single point. This is the reason why the control of the staffing level s needs to be delicate (and requires a square-root staffing rule) to achieve QED for the original Erlang A model; as pointed out by [3], a small change in traffic intensity $R/s (= \lambda/(s\mu))$ due to changes in parameters (λ , μ , and s) can incur a large change in the delay probability P_Q (and thus changes the regime the system belongs to). However, such a delicate control may not be necessary since we know that there exists a wider QED region above the no intervention line ($R = R_Q$) in phase diagrams. In other words, we can expand the QED regime by implementing the CBC scheme to make $R_Q < R$, avoiding the operation of large systems at a singular point $s \approx R = R_Q$. For practitioners struggling to maintain stable operation of large-scale abandonment systems in the QED regime, it would be easier to control ε and τ appropriately to realize $R_Q < R$ and make systems robust, than to constantly control s around $R = R_Q$ following the conventional or refined square-root staffing rules.

6. Numerical Experiments

In this section we demonstrate the precision of our non-asymptotic normal approximation, identify the source of discrepancies between non-asymptotic and asymptotic approximations, and observe the robustness of the system with customer abandonment under the CBC scheme.

6.1. Comparison among Exact Result and Non-Asymptotic/Asymptotic Approximations

We first discuss the $R = R_Q$ case. Specifically, we consider the original Erlang A ($\varepsilon = \tau = 0$) case since the popular square-root staffing rule is available. (Note: Our asymptotic representation of P_Q for the $\varepsilon = \tau = 0$ case is identical to the popular square-root staffing rule for the original Erlang A model: $P_Q = \phi(c)$, where $\phi(c)$ is defined in Equation (22). See also Table 8.) Table 9 shows the difference between the exact staffing levels and the staffing levels derived from the non-asymptotic staffing rule (Proposition 2) and the square-root staffing rule for the original Erlang A model. The staffing levels derived from the non-asymptotic staffing rule usually agree with the exact staffing levels with a difference of at most 1 at all levels of γ , while the staffing levels derived from the square-root staffing rule disagree with the exact staffing levels by two or more when $\gamma = 10$.

Table 9: Staffing levels to meet the target P_Q following the exact, non-asymptotic, and square-root staffing rules ($R = R_Q$ case).

γ	Target P_Q level (α)	Exact Staffing Level (s)	Difference from Exact Staffing Level	
			Non-Asymptotic	Square-root Staffing
10	95%	20	-1	-8
	83%	30	0	-5
	60%	40	+1	-2
	30%	50	0	-2
1	95%	40	-1	-1
	83%	44	0	0
	60%	49	0	+1
	30%	55	0	-1
0.1	95%	48	0	0
	83%	50	0	0
	60%	52	0	0
	30%	56	0	0

Notes: $\lambda = 50$, $\mu = 1$, $\varepsilon = \tau = 0$, $R = R_Q = 50$

Figure 4 compares the numerical results of the non-asymptotic and square-root staffing approximations with the exact values using the same parameters shown in Figure 4 of [1]. As [1] show, the square-root staffing approximation matches well with the exact values at $\gamma = 0.1$ and $\gamma = 1$, but not at $\gamma = 10$. In contrast, our non-asymptotic approximation traces the exact values for all cases.

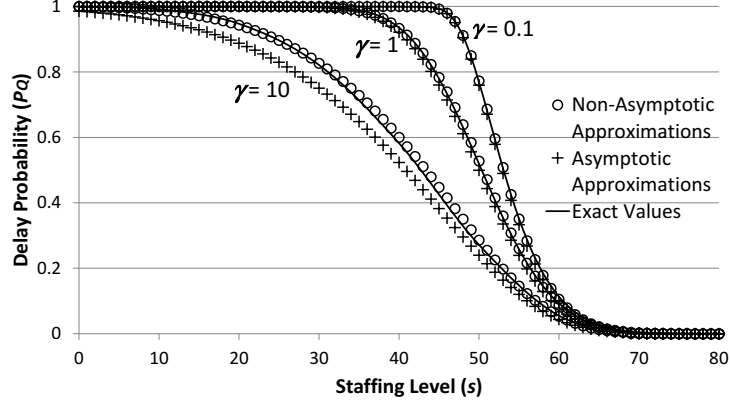


Figure 4: Comparison between the exact values and non-asymptotic/square-root staffing approximations of P_Q ($R = R_Q$ case). Notes: $\lambda = 50$, $\mu = 1$, $\varepsilon = \tau = 0$, $R = R_Q = 50$.

Figure 5 shows the difference of the delay probability (P_Q) between our non-asymptotic approximation and the square-root staffing rule. This difference is primarily accounted for by the term π_s , which only appears in the non-asymptotic representation of P_Q (except for the continuity correction terms Δ and Δ' , whose contributions are smaller than π_s). (See the Appendix for the derivation.) The discrepancy term π_s could become large when R is small and γ is large, in which case P_Q of the square-root staffing rule could have a larger error. On the other hand, in the asymptotic limit of a large R , both π_s and the continuity correction terms are regarded as negligible (because no discreteness exists), in which case the square-root staffing rule becomes precise.

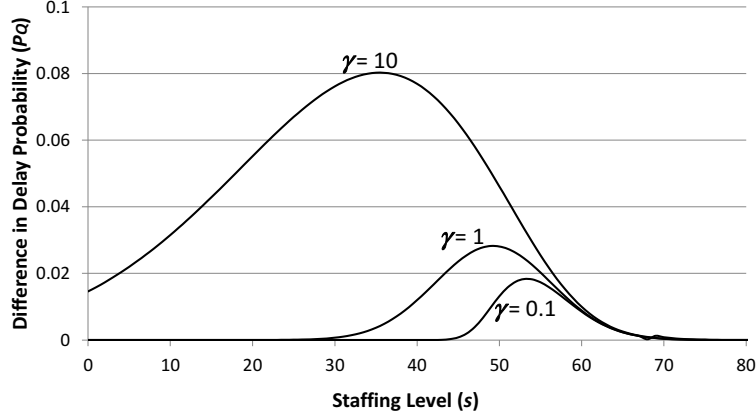


Figure 5: Impact of reneging rate γ on the *difference* between non-asymptotic and square-root staffing approximations of P_Q ($R = R_Q$ case). *Notes:* $\lambda = 50$, $\mu = 1$, $\varepsilon = \tau = 0$, $R = R_Q = 50$. Ripples at around $s = 69$ are due to numerical inaccuracy.

Figure 6 shows that as R increases, the non-asymptotic approximation approaches the asymptotic approximation, as expected.

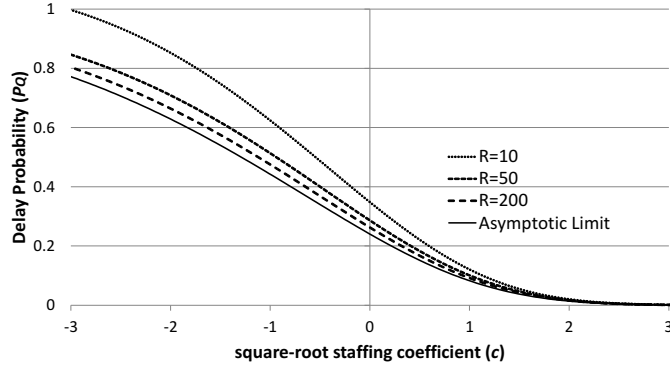


Figure 6: Comparison between non-asymptotic and asymptotic approximations of P_Q (square-root scale; $R = R_Q$ case). *Notes:* $\mu = 1$, $\gamma = 10$, $\lambda = R = 10, 50, 200$, and $\varepsilon = \tau = 0$.

Next, we compare the exact values of P_Q with non-asymptotic approximations of P_Q when $R \neq R_Q$ ($\varepsilon + \tau \neq 0$). Table 10 shows both absolute error (denoted as Abs.; defined as $|exact - approximation|$) and relative error (denoted as Rel.; defined as $(exact - approximation)/exact$ in %). Note that we

only consider non-asymptotic approximation in this table since the square-root staffing rule is not applicable when $R \neq R_Q$ and the linear staffing approximation is crude to compare with the exact values. Table 10 demonstrates that our non-asymptotic approximation is accurate for a wide range of s (from the ED to the QD regime). We observe a larger relative error for a larger s ($> R = 50$); however, this is not important since this large relative error is caused by P_Q approaching zero as s increases.

Table 10: Comparison between the exact results and non-asymptotic approximations of P_Q .

ε, τ	s	20	30	40	50	60	70	80	Average	Max
0, 0	Exact	1.00	1.00	0.94	0.52	0.09	0.00	0.00	0.002	0.009
	Non-Asym	1.00	1.00	0.93	0.53	0.09	0.00	0.00		
	Abs.	0.00	0.00	0.00	0.01	0.00	0.00	0.00		
	Rel.%	0.00	0.07	0.22	-1.79	5.15	37.37	76.73		
0, 0.2	Exact	1.00	0.99	0.79	0.35	0.06	0.00	0.00	0.003	0.008
	Non-Asym	1.00	0.99	0.80	0.36	0.06	0.00	0.00		
	Abs.	0.00	0.00	0.01	0.01	0.00	0.00	0.00		
	Rel.%	0.00	0.18	-0.92	-2.38	5.89	37.70	76.80		
0.2, 0	Exact	1.00	0.97	0.73	0.32	0.06	0.00	0.00	0.003	0.010
	Non-Asym	1.00	0.97	0.74	0.33	0.05	0.00	0.00		
	Abs.	0.00	0.00	0.01	0.01	0.00	0.00	0.00		
	Rel.%	0.02	0.19	-1.34	-2.56	5.86	37.66	76.79		
0.2, 0.2	Exact	1.00	0.91	0.59	0.24	0.05	0.00	0.00	0.003	0.012
	Non-Asym	1.00	0.91	0.61	0.25	0.04	0.00	0.00		
	Abs.	0.00	0.00	0.01	0.01	0.00	0.00	0.00		
	Rel.%	0.07	-0.32	-2.03	-2.32	6.34	37.86	86.37		
0.2, 0.5	Exact	0.99	0.80	0.48	0.20	0.04	0.00	0.00	0.003	0.011
	Non-Asym	0.99	0.81	0.49	0.20	0.03	0.00	0.00		
	Abs.	0.00	0.01	0.01	0.00	0.00	0.00	0.00		
	Rel.%	0.08	-1.07	-2.19	-2.04	8.81	38.19	76.92		
0.5, 0.2	Exact	0.92	0.68	0.40	0.16	0.03	0.00	0.00	0.005	0.012
	Non-Asym	0.93	0.69	0.41	0.17	0.02	0.00	0.00		
	Abs.	0.00	0.01	0.01	0.00	0.01	0.00	0.00		
	Rel.%	-0.45	-1.60	-2.37	-2.02	37.96	38.19	76.92		

Notes: $\lambda = 50$, $\mu = 1$, $R = 50$. Note that $R \neq R_Q$ except for the first case ($\varepsilon = \tau = 0$).

6.2. Robustness of the Modified Erlang A Model

In this final subsection, we discuss how the CBC scheme—blocking arrivals (ε) and increasing service rate (τ)—affects the robustness of the modified Erlang A system. We first observe the impacts of ε and τ on P_Q when fixing the size of the system. Figure 7 shows that ε has larger impact on P_Q than τ , partly due to the higher marginal reduction of $R_Q = \frac{1-\varepsilon}{1+\tau}R$ for ε than τ . This result is consistent with our intuition that blocking arrivals is more effective than increasing service rates of servers.

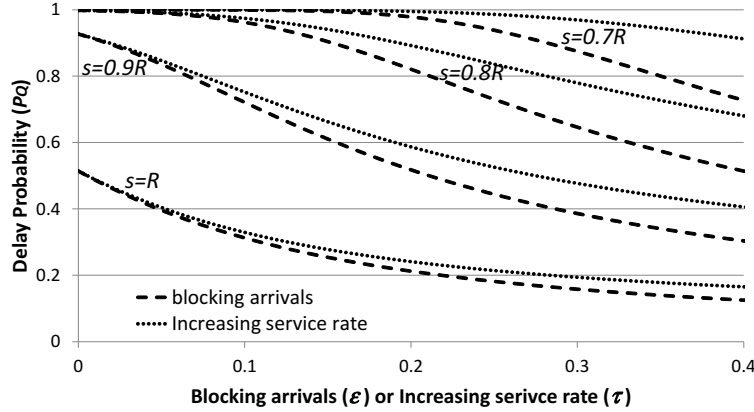


Figure 7: Comparison between the impacts of blocking arrivals (ε) and increasing service rate (τ). Notes: $\mu = 1$, $\gamma = 1$, $\lambda = R = 200$, and $s/R = 0.7, 0.8, 0.9, 1$.

We next fix the CBC scheme parameters (ε and τ) and examine the robustness of systems by changing their sizes. Specifically, we change two parameters, either s or λ , and plot P_Q values; a flatter P_Q line implies that a system is more robust. We first alter the staffing level s while fixing other parameters and observe the P_Q plots. Figures 8 and 9 correspond to the modified Erlang A models with no intervention ($\varepsilon = \tau = 0$) and with intervention ($\varepsilon = 0.1, \tau = 0.05$), respectively. Notice that the asymptotic lines of P_Q are different in these two figures: In Figure 8 ($R_Q = R$ case), P_Q approaches a step function at $s = R$ as R increases, indicating that the system operating in a QED regime is very sensitive to parameters, while in Figure 9 ($R_Q < R$ case), P_Q approaches a linear

asymptotic line $P_Q = \frac{1 - \frac{s}{R}}{1 - \frac{s}{R_Q}} = \frac{1 + \tau}{\varepsilon + \tau} \left(1 - \frac{s}{R}\right)$ for $\frac{R_Q}{R} \leq \frac{s}{R} \leq 1$ as R increases. These two different asymptotic lines for P_Q are presented in Table 8. Note that in Table 8, only a square-root staffing representation (using c) is presented for the $R = R_Q$ case; however, this square-root asymptotic line approaches a step function at $s = R$ in the limit of large R . The comparison of the two asymptotic lines indicates that the CBC scheme ($R_Q < R$) makes the system more robust to changes in parameters (s for this case) in order to maintain P_Q in a QED regime.

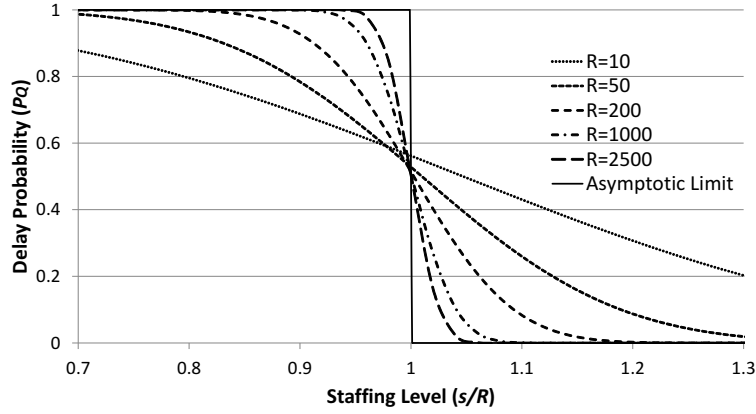


Figure 8: Impact of change in s/R on P_Q (linear scale; $R = R_Q$ case). Notes: $\mu = 1$, $\gamma = 1$, $\varepsilon = \tau = 0$, and $\lambda = R = 10, 50, 200, 1000, 2500$.

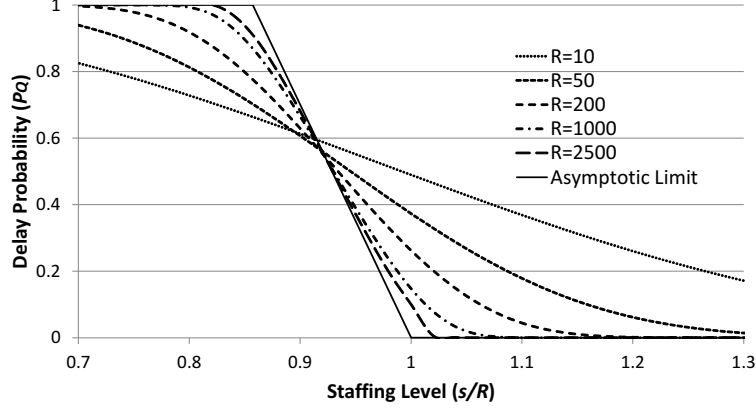


Figure 9: Impact of change in s/R on P_Q (linear scale; $R_Q < R$ case). Notes: $\mu = 1$, $\gamma = 1$, $\varepsilon = 0.1$, $\tau = 0.05$, and $\lambda = R = 10, 50, 200, 1000, 2500$.

Finally, we observe the impact of traffic intensity $R/s (= \lambda/(s\mu))$ on P_Q by changing λ (while fixing s and μ). Figure 10 compares no intervention ($R_Q = R$; $\varepsilon = \tau = 0$) and intervention ($R_Q < R$; $\varepsilon = 0$, $\tau = 0.1, 0.2$) cases. The figure shows how P_Q responds to the change in λ while fixing other parameters (i.e., we control λ to vary R/s to draw each line): If the P_Q line is flatter, the system is more robust to the change in λ . Figure 10 shows that smaller systems are proportionally less sensitive to changes in λ (note that we fix μ in this figure), while for larger service systems, it is important to control (i.e., lower) R_Q , enabling the system to operate in a wider region of a QED regime. Asymptotic lines indicated in Figure 10 are: a step function at $\frac{R}{s} = 1$ for the $\tau = 0$ case and close-to-linear lines $P_Q = \frac{1 - \frac{s}{R}}{1 - \frac{R_Q}{R}} = \frac{1 + \tau}{\varepsilon + \tau} \frac{\frac{R}{s} - 1}{\frac{R}{s}} (\approx \frac{1 + \tau}{\varepsilon + \tau} (\frac{R}{s} - 1))$ at $1 \leq \frac{R}{s} \leq \frac{R}{R_Q} (= \frac{1 + \tau}{1 - \varepsilon})$ for the $\tau = 0.1, 0.2$ cases (see Table 8).

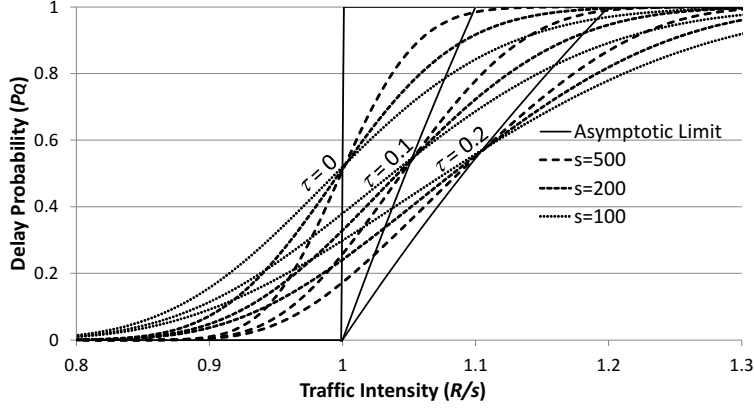


Figure 10: Impact of change in R/s on P_Q (linear scale). Notes: $\mu = 1$, $\gamma = 1$, $\varepsilon = 0$, $\tau = 0, 0.1, 0.2$, $R/s = \lambda/s$, and $s = 100, 200, 500$.

7. Conclusion

In this paper we study a modified Erlang A model, which allows arrival and service rates to change when systems are congested—we call this intervention the congestion-based control (CBC) scheme. We derive non-asymptotic and asymptotic normal representations for the quality of service (QoS) performance indicators: Non-asymptotic formulae provide easy-to-calculate yet accurate results for systems of both small and large sizes, while asymptotic formulae provide insight into the QoS levels of very large systems. Specifically, by drawing the three distinct asymptotic regimes (ED, QD, and QED) in a phase diagram, we reveal that the highly sensitive QoS properties of systems with customer abandonment can be attributed to operation at the point of singularity where the three regimes co-exist. We demonstrate that the CBC scheme can avoid this point of singularity, and thus achieve a more robust system that is less sensitive to changes in parameters.

For the analysis of the modified Erlang A model under the CBC scheme, we utilize the Markov chain decomposition method [26]. This method allows us to decompose a complex Markov chain into simpler sub-chains, which are then analyzed individually; this way, we can treat each sub-system precisely while still

maintaining the key properties (such as the resource requirement) of each sub-system in the final representation of performance indicators. In fact, the explicit dependence of the asymptotic QoS indicators on each decomposed sub-chain is easy to derive thanks to the Markov chain decomposition method. We believe that our methodology to derive the results in this study can be instrumental in understanding the properties of other complicated Markov chain models.

References

- [1] O. Garnett, A. Mandelbaum, M. Reiman, Designing a call center with impatient customers, *Manufacturing & Service Operations Management* 4 (3) (2002) 208–227.
- [2] A. Mandelbaum, S. Zeltyn, The Palm/Erlang-A queue, with applications to call centers, *Faculty of Industrial Engineering & Management, Technion, Haifa, Israel* (2005).
- [3] W. Whitt, Sensitivity of performance in the Erlang-A queueing model to changes in the model parameters, *Operations Research* 54 (2) (2006) 247–260.
- [4] R. C. A. Palm, Research on telephone traffic carried by full availability groups, *Tele*, 1957.
- [5] K. Udagawa, G. Nakamura, On a Queue in which Joining Customers Give up Their Services Halfway, *J. Ops. Res. Japan* 1 (1957) 59–76.
- [6] F. A. Haight, Queueing with reneging, *Metrika* 2 (1) (1959) 186–197.
- [7] C. Ancker, A. Gafarian, Some queueing problems with balking and reneging. I, *Operations Research* 11 (1) (1963) 88–100.
- [8] R. C. Larson, K. Sasanuma, Congestion pricing: A Parking queue model, *Journal of Industrial and Systems Engineering* 4 (1) (2010) 1–17.
- [9] E. H. Kaplan, Analyzing tenant assignment policies, *Management Science* 33 (3) (1987) 395–408.
- [10] S. A. Zenios, Modeling the transplant waiting list: a queueing model with reneging, *Queueing systems* 31 (3-4) (1999) 239–251.
- [11] S. Halfin, W. Whitt, Heavy-traffic limits for queues with many exponential servers, *Operations research* 29 (3) (1981) 567–588.

- [12] N. Gans, G. Koole, A. Mandelbaum, Telephone call centers: Tutorial, review, and research prospects, *Manufacturing & Service Operations Management* 5 (2) (2003) 79–141.
- [13] S. Borst, A. Mandelbaum, M. I. Reiman, Dimensioning large call centers, *Operations research* 52 (1) (2004) 17–34.
- [14] A. Bassamboo, J. M. Harrison, A. Zeevi, Design and control of a large call center: Asymptotic analysis of an LP-based method, *Operations Research* 54 (3) (2006) 419–435.
- [15] I. Gurvich, M. Armony, A. Mandelbaum, Service-level differentiation in call centers with fully flexible servers, *Management Science* 54 (2) (2008) 279–294.
- [16] A. Mandelbaum, S. Zeltyn, Staffing many-server queues with impatient customers: Constraint satisfaction in call centers, *Operations Research* 57 (5) (2009) 1189–1205.
- [17] B. Zhang, J. S. van Leeuwen, B. Zwart, Staffing call centers with impatient customers: Refinements to many-server asymptotics, *Operations Research* 60 (2) (2012) 461–474.
- [18] J. Dai, S. He, Many-server queues with customer abandonment: A survey of diffusion and fluid approximations, *Journal of Systems Science and Systems Engineering* 21 (1) (2012) 1–36.
- [19] I. Gurvich, J. Huang, A. Mandelbaum, Excursion-based universal approximations for the Erlang-A queue in steady-state, *Mathematics of Operations Research* (2013).
- [20] T. B. Crabill, D. Gross, M. J. Magazine, A classified bibliography of research on optimal design and control of queues, *Operations Research* 25 (2) (1977) 219–232.

- [21] Z. Feldman, A. Mandelbaum, W. A. Massey, W. Whitt, Staffing of time-varying queues to achieve time-stable performance, *Management Science* 54 (2) (2008) 324–338.
- [22] Y. L. Koçağa, A. R. Ward, Admission control for a multi-server queue with abandonment, *Queueing Systems* 65 (3) (2010) 275–323.
- [23] J. Sanders, S. Borst, A. Janssen, J. v. Leeuwaarden, Optimal admission control for many-server systems with QED-driven revenues, *Stochastic Systems* 7 (2) (2017) 315–341.
- [24] A. P. Ghosh, A. P. Weerasinghe, Optimal buffer size and dynamic rate control for a queueing system with impatient customers in heavy traffic, *Stochastic Processes and Their Applications* 120 (11) (2010) 2103–2141.
- [25] Y. L. Koçağa, An approximating diffusion control problem for dynamic admission and service rate control in a $g/m/n+g$ queue, *Operations Research Letters* 45 (6) (2017) 538–542.
- [26] K. Sasanuma, R. Hampshire, A. Scheller-Wolf, Markov chain decomposition based on total expectation theorem, *arXiv preprint arXiv:1901.06780* (2019).
- [27] K. Sasanuma, A. Scheller-Wolf, Approximate performance measures for a single station two-stage reneging queue, *Operations Research Letters* 49 (2) (2021) 212–217.
- [28] K. Sasanuma, Asymptotic analysis for systems with deferred abandonment, *Mathematics* 9 (18) (2021) 2187.
- [29] D. Braess, A. Nagurney, T. Wakolbinger, On a paradox of traffic planning, *Transportation science* 39 (4) (2005) 446–450.
- [30] M. Pinedo, *Scheduling: theory, algorithms, and systems*, Springer, 2012.
- [31] H. C. Tijms, *A First Course in Stochastic Models*, John Wiley & Sons, 2003.

- [32] M. Harchol-Balter, Performance Modeling and Design of Computer Systems: Queueing Theory in Action, Cambridge University Press, 2013.
- [33] E. B. Wilson, M. M. Hilferty, The Distribution of Chi-Square, Proceedings of the National Academy of Sciences 17 (12) (1931) 684–688.
- [34] S. M. Lesch, D. R. Jeske, Some suggestions for teaching about normal approximations to Poisson and binomial distribution functions, The American Statistician 63 (3) (2009) 274–277.

Appendix

Appendix A Proofs

Proof of Lemma 1. We first prove Equations (1) and (2). Note that from Corollary 1.10. in [1], $\pi_s^i = \Pr\{\# \text{ of customers} = s \mid \text{system is in sub-chain } i\} = \pi_s / P_i$, where the state s is in sub-chain i . Therefore, $P_i = \pi_s / \pi_s^i$ holds for sub-chain $i (= 1, 2)$. Using this result and the property that both sub-chains overlap at a single state s , we have

$$1 = \sum_{i=1}^2 P_i - \pi_s = \sum_{i=1}^2 \frac{\pi_s}{\pi_s^i} - \pi_s = \pi_s \cdot \left(\sum_{i=1}^2 \frac{1}{\pi_s^i} - 1 \right),$$

from which we obtain Equations (1) and (2).

In the derivation above, we use the fact from [1] that the sub-chain's steady-state probability is equal to the conditional steady-state probability of the full Markov chain (MC). However, this assumption is not trivial. For our model, this holds because the modified Erlang A MC is reversible. If it is not reversible, we need to decompose the MC more carefully to ensure the steady-state probabilities of sub-chains equal the conditional steady-state probabilities of the full chain.

We next derive Equations (3) and (4). From the flow balance condition, the total arrival rate λ should be equal to the sum of the average number of customers being serviced per unit time and the average number of customers reneging/balking per unit time. Using this condition, the average number of customers being serviced given that a state is in sub-chain 2, is calculated as $0 \cdot \pi_s^2 + s\mu_Q \cdot (1 - \pi_s^2) = s\mu_Q \cdot (1 - \pi_s^2)$ because the departure rate $s\mu_Q$ only exists when the system (sub-chain 2) is busy. Therefore, the proportion of reneging/balking customers among the total arriving customers given in sub-chain 2 is

$$\frac{\lambda - s\mu_Q \cdot (1 - \pi_s^2)}{\lambda} = \pi_s^2 + \left(1 - \frac{s\mu_Q}{\lambda}\right) (1 - \pi_s^2) = \frac{1 + (1 - \frac{s\mu_Q}{\lambda})(\frac{1}{\pi_s^2} - 1)}{\frac{1}{\pi_s^2}} = \frac{1 + p \cdot (\frac{1}{\pi_s^2} - 1)}{\frac{1}{\pi_s^2}},$$

where $p = 1 - (s\mu_Q/\lambda) = 1 - (1 + \tau)(s\mu/\lambda) = 1 - (1 + \tau)(a + 1)$. (Note that $s\mu/\lambda = s/R = a + 1$ from the definition of the linear coefficient a .) This proportion is equivalent to the conditional probability of abandonment given in

sub-chain 2:

$$P_{ab}^2 = \frac{1 + p \cdot (\frac{1}{\pi_s^2} - 1)}{\frac{1}{\pi_s^2}}.$$

Hence, using the total probability theorem, Equations (3) and (4) are proved as

$$P_{ab} = P_{ab}^2 \cdot P_Q = \frac{1 + p \cdot (\frac{1}{\pi_s^2} - 1)}{\frac{1}{\pi_s^2}} P_Q = \frac{1 + p \cdot (\frac{1}{\pi_s^2} - 1)}{\frac{1}{\pi_s^2} + \frac{1}{\pi_s^2} - 1}.$$

Next, we show Equations (5) and (6). Equation (5) is obtained from the flow balance requirement: $\lambda P_{ab} = \gamma L_Q + \varepsilon \lambda P_Q$ for reneging systems and $\lambda P_{ab} = \delta L_Q + \varepsilon \lambda P_Q$ for balking systems. (Note that $\delta \cdot L_Q = \delta \cdot (\sum_{k=0}^u k \pi_{s+k}) = \sum_{k=0}^u (\delta k) \pi_{s+k}$ is the average number of balking customers, where we define $u = \lfloor \lambda_Q / \delta \rfloor$; at states greater than $s + u$ no customer enters the system and all arrivals balk.) Equation (6) is obtained by plugging Equations (2) and (4) into Equation (5). \square

Remark A.1. *The average delay time can also be represented by the blocking probabilities. For the reneging (or balking) system, we have the following expressions, respectively:*

$$W_Q = \frac{1}{\gamma} \cdot \frac{P_{ab} - \varepsilon P_Q}{1 - \varepsilon P_Q} = \frac{1}{\gamma} \cdot \frac{(1 - \varepsilon) + (p - \varepsilon)(\frac{1}{\pi_s^2} - 1)}{(\frac{1}{\pi_s^2} - \varepsilon) + (1 - \varepsilon)(\frac{1}{\pi_s^2} - 1)}$$

or

$$W_Q = \frac{1}{\delta} \cdot \frac{P_{ab} - \varepsilon P_Q}{1 - P_{ab}} = \frac{1}{\delta} \cdot \frac{(1 - \varepsilon) + (p - \varepsilon)(\frac{1}{\pi_s^2} - 1)}{(\frac{1}{\pi_s^2} - 1) + (1 - p)(\frac{1}{\pi_s^2} - 1)}.$$

These formulae can be proved by Little's law, $L_Q = \lambda_{\text{eff}} W_Q$, where the effective arrival rate for reneging systems and balking systems are $\lambda_{\text{eff}} = \lambda \cdot (1 - P_Q) + \lambda_Q P_Q = \lambda \cdot (1 - P_Q) + (1 - \varepsilon) \lambda P_Q = \lambda \cdot (1 - \varepsilon P_Q)$ and $\lambda_{\text{eff}} = \lambda \cdot (1 - P_{ab})$, respectively.

Proof of Corollary 1. We denote π_s^1 as P_{block} . Using Equation (2), we obtain

$$\frac{1}{\pi_s^2} = \frac{P_Q}{1 - P_Q} \cdot \frac{1 - P_{\text{block}}}{P_{\text{block}}}$$

and equivalently

$$\frac{1}{\pi_s^2} - 1 = \frac{P_Q - P_{block}}{(1 - P_Q) P_{block}}.$$

By plugging these two equations into Equation (3), we obtain Equation (8). \square

Proof of Corollary 2. The first part of Corollary 2 may be obvious intuitively: P_Q decreases as any of the abandonment-related parameters increase. To prove this result, note that $1/\pi_s^2 = 1 + \sum_{k=1}^{\infty} \prod_{i=0}^{k-1} (\lambda_{s+i}/\mu_{s+i+1})$ (Equation (3.12) in [2]), where λ_k and μ_k for $k \geq s$ are defined in Section 3.1. An increase in one of the abandonment-related parameters (γ , δ , and ε) always leads to a reduction in λ_k or an increase in μ_k , reducing $1/\pi_s^2$, while $(1/\pi_s^2) - 1$ remains positive and constant. From Equation (2), we conclude that P_Q decreases as any of the abandonment-related parameters increase. For the second part, assume that all performance-related parameters (s , λ , μ , and τ) are fixed, and hence, p ($= 1 - s\mu_Q/\lambda$) and P_{block} are fixed as well. In this case, P_Q and P_{ab} are the only indicators that depend on abandonment-related parameters. If $p < P_{block}$ ($p > P_{block}$) holds, Equation (8) shows there exists (does not exist) a trade-off between P_Q and P_{ab} , respectively. Combining this result with the first part of this corollary, we can derive the second part. \square

Remark A.2. *Examples of both $p < P_{block}$ and $p > P_{block}$ cases are easy to find: If $s\mu_Q$ is larger than λ , p becomes negative and $p < P_{block}$ holds; in contrast, if $s\mu_Q$ is much smaller than λ , p becomes close to 1 and $p > P_{block}$ holds. From our non-asymptotic approximation, we can see that non-negative τ is typically a sufficient condition for $p < P_{block}$ to hold, and also that negative τ is often a necessary condition for $p > P_{block}$ to hold.*

Proof of Lemma 2. We discuss each sub-chain separately. Define R.V.'s and parameters as in Table 2. Assume s , s' , and s'' are non-negative integers.

1. M/M/s/s sub-chain (left sub-chain): This result is shown in [3].

For all $k = 0, 1, 2, \dots, s$,

$$\begin{aligned}\pi_k^1 &= \pi_{k+1}^1 \frac{(k+1)\mu}{\lambda} = \pi_{k+1}^1 \frac{k+1}{R} = \dots = \pi_s^1 \frac{(k+1)(k+2) \cdots s}{R^{s-k}} \\ &= \pi_s^1 \frac{s!}{k!} \frac{R^k}{R^s} = \pi_s^1 \frac{e^{-R} R^k / k!}{e^{-R} R^s / s!} = \pi_s^1 \frac{\Pr\{X_P = k\}}{\Pr\{X_P = s\}}.\end{aligned}$$

By summing up the terms with respect to k and applying the normalization condition, we obtain

$$\frac{1}{\pi_s^1} = \frac{\Pr\{X_P \leq s\}}{\Pr\{X_P = s\}} = \frac{F_P(s; R)}{f_P(s; R)}.$$

We can confirm that this result matches the Erlang Loss (Erlang B) formula:

$$\frac{1}{\pi_s^1} = \frac{\sum_{k=0}^s (\lambda/\mu)^k / k!}{(\lambda/\mu)^s / s!}.$$

2. Reneging sub-chain (right sub-chain):

For all $k = 0, 1, 2, \dots$,

$$\begin{aligned}\pi_{s+k}^2 &= \pi_{s+k-1}^2 \frac{\lambda_Q}{s\mu_Q + k\gamma} = \pi_{s+k-1}^2 \frac{(\lambda_Q/\gamma)}{(s\mu_Q/\gamma) + k} = \pi_{s+k-1}^2 \frac{R'}{s' + k} \\ &= \pi_{s+k-2}^2 \frac{R'}{s' + k} \cdot \frac{R'}{s' + k - 1} = \dots = \pi_s^2 \frac{R'^k}{(s' + 1)(s' + 2) \cdots (s' + k)} \\ &= \pi_s^2 \frac{e^{-R'} R'^{s'+k} / (s' + k)!}{e^{-R'} R'^{s'} / s'!} = \pi_s^2 \frac{\Pr\{X'_P = s' + k\}}{\Pr\{X'_P = s'\}}.\end{aligned}$$

By summing up the terms with respect to k and applying the normalization condition, we obtain

$$\frac{1}{\pi_s^2} = \frac{\Pr\{X'_P \geq s'\}}{\Pr\{X'_P = s'\}}.$$

We further rewrite this representation using the Poisson PMF/CDF:

$$\begin{aligned}\frac{1}{\pi_s^2} &= \frac{\Pr\{X'_P \geq s'\}}{\Pr\{X'_P = s'\}} = \frac{\Pr\{X'_P = s'\}}{\Pr\{X'_P = s'\}} + \frac{\Pr\{X'_P \geq s' + 1\}}{\Pr\{X'_P = s'\}} \\ &= 1 + \frac{1 - \Pr\{X'_P \leq s'\}}{\Pr\{X'_P = s'\}} = 1 + \frac{1 - F_P(s'; R')}{f_P(s'; R')}.\end{aligned}$$

3. Balking sub-chain (alternate right sub-chain):

For all $k = 0, 1, 2, \dots, s''$,

$$\begin{aligned}
\pi_{s+k}^2 &= \pi_{s+k-1}^2 \frac{\lambda_Q - (k-1)\delta}{s\mu_Q} = \pi_{s+k-1}^2 \frac{(\lambda_Q/\delta) - (k-1)}{(s\mu_Q/\delta)} \\
&= \pi_{s+k-1}^2 \frac{s'' - (k-1)}{R''} = \dots = \pi_s^2 \frac{(s'' - k + 1) \cdots (s'' - 1)s''}{R''^k} \\
&= \pi_s^2 \frac{e^{-R''} R''^{s''-k} / (s'' - k)!}{e^{-R''} R''^{s''} / s''!} = \pi_s^2 \frac{\Pr\{X''_P = s'' - k\}}{\Pr\{X''_P = s''\}}.
\end{aligned}$$

By summing up the terms with respect to k and applying the normalization condition, we obtain

$$\frac{1}{\pi_s^2} = \frac{\Pr\{X''_P \leq s''\}}{\Pr\{X''_P = s''\}} = \frac{F_P(s''; R'')}{f_P(s''; R'')}.$$

□

Proof of Proposition 1.

1. Poisson CDF to standard normal CDF:

We first make a discrete-to-continuous conversion from Poisson to normal with a continuity correction “+0.5”. We then convert normal to standard normal using $c_{s;R}$ and Δ_R :

$$F_P(s; R) \approx F_N(s + 0.5; R, \sqrt{R}) = \Phi\left(\frac{(s + 0.5) - R}{\sqrt{R}}\right) = \Phi(c_{s;R} + \Delta_R).$$

2. Poisson PMF to standard normal PDF:

Using the result above and the assumption that Δ_R is sufficiently small, we obtain

$$\begin{aligned}
f_P(s; R) &= F_P(s; R) - F_P(s-1; R) \approx F_N(s + 0.5; R, \sqrt{R}) - F_N(s - 0.5; R, \sqrt{R}) \\
&\approx \Phi(c_{s;R} + \Delta_R) - \Phi(c_{s;R} - \Delta_R) \approx 2\phi(c_{s;R} + \Delta_R)\Delta_R \\
&= \frac{\phi(c_{s;R} + \Delta_R)}{\sqrt{R}} = \frac{a_{s;R} \cdot \phi(c_{s;R} + \Delta_R)}{c_{s;R}}.
\end{aligned}$$

3. Poisson modified hazard function to standard normal hazard function:

Using the above results and the definition of the hazard function for the standard normal distribution, it is straightforward to derive the following:

$$\begin{aligned}
\frac{f_P(s; R)}{1 - F_P(s; R)} &\approx \frac{\phi(c_{s;R} + \Delta_R)}{\sqrt{R} \cdot (1 - \Phi(c_{s;R} + \Delta_R))} = \frac{h(c_{s;R} + \Delta_R)}{\sqrt{R}} = \frac{a_{s;R} \cdot h(c_{s;R} + \Delta_R)}{c_{s;R}} \\
\frac{f_P(s; R)}{F_P(s; R)} &\approx \frac{\phi(c_{s;R} + \Delta_R)}{\sqrt{R} \cdot \Phi(c_{s;R} + \Delta_R)} = \frac{h(-c_{s;R} - \Delta_R)}{\sqrt{R}} = \frac{a_{s;R} \cdot h(-c_{s;R} - \Delta_R)}{c_{s;R}}.
\end{aligned}$$

□

Proof of Proposition 2. Without calculation, the uniqueness and the existence of the solution can be inferred from the physical property of the model: If the number of staff increases from 0 to infinity, the exact as well as the non-asymptotic representation of P_Q and P_{ab} monotonically (strictly) decrease from 1 to 0. The non-asymptotic representation of P_Q and P_{ab} that satisfy such a property must have a unique solution to $P_Q = \alpha$ or $P_{ab} = \alpha$ for any $\alpha \in (0, 1)$. The ceiling of the solution needs to be taken to obtain the optimal staffing level because a staffing level should be an integer whereas a solution (staffing coefficients c or a) is not. □

Appendix B Exact Representation of Performance Indicators for the Modified Erlang A Reneging Model

The Poisson representation of performance indicators is exact but only for a set of parameters that satisfies integer constraints for staffing levels of the second (reneging/balking) sub-chain. If we want to know exact solutions for a general set of parameters, we should use the exact representation of the blocking probability of the sub-chain we are interested in. For a reneging sub-chain, the blocking probability is known as

$$\frac{1}{\pi_s^2} = \frac{s\mu_Q}{\gamma} \int_0^1 e^{\lambda_Q t/\gamma} (1-t)^{\lambda_Q t/\gamma-1} dt.$$

Proof. We follow [4]. Using gamma and beta functions, for $k = 0, 1, 2, \dots$,

$$\begin{aligned} \pi_{s+k}^2 &= \pi_{s+k-1}^2 \frac{\lambda_Q}{s\mu_Q + k\gamma} = \dots = \pi_s^2 (\lambda_Q/\gamma)^k (s\mu_Q/\gamma) \frac{1}{(s\mu_Q/\gamma)(s\mu_Q/\gamma+1) \cdots (s\mu_Q/\gamma+k)} \\ &= \pi_s^2 (s\mu_Q/\gamma) \frac{(\lambda_Q/\gamma)^k \Gamma(s\mu_Q/\gamma) \Gamma(k+1)}{k! \Gamma(s\mu_Q/\gamma+k+1)} = \pi_s^2 \frac{(\lambda_Q/\gamma)^k}{k!} B(s\mu_Q/\gamma, k+1) \\ &= \pi_s^2 (s\mu_Q/\gamma) \frac{(\lambda_Q/\gamma)^k}{k!} \int_0^1 t^k (1-t)^{s\mu_Q/\gamma-1} dt = \pi_s^2 (s\mu_Q/\gamma) \int_0^1 \frac{(\lambda_Q t/\gamma)^k}{k!} (1-t)^{s\mu_Q/\gamma-1} dt. \end{aligned}$$

From the normalization condition,

$$\begin{aligned}
1 &= \sum_{k=0}^{\infty} \pi_{s+k}^2 = \pi_s^2 (s\mu_Q/\gamma) \int_0^1 \left(\sum_{k=0}^{\infty} \frac{(\lambda_Q t/\gamma)^k e^{-\lambda_Q t/\gamma}}{k!} \right) e^{\lambda_Q t/\gamma} (1-t)^{\lambda_Q t/\gamma-1} dt \\
&= \pi_s^2 \cdot \frac{s\mu_Q}{\gamma} \int_0^1 e^{\lambda_Q t/\gamma} (1-t)^{\lambda_Q t/\gamma-1} dt.
\end{aligned}$$

□

Together with the exact solution (Erlang Loss formula) for the left sub-chain (an M/M/s/s queue), which is

$$\frac{1}{\pi_s^1} = \frac{\sum_{i=0}^s (\lambda/\mu)^i / i!}{(\lambda/\mu)^s / s!} = \frac{\sum_{i=0}^s e^{-\lambda/\mu} (\lambda/\mu)^i / i!}{e^{-\lambda/\mu} (\lambda/\mu)^s / s!} = \frac{\Pr\{X_P \leq s\}}{\Pr\{X_P = s\}},$$

we can derive the exact representation of performance indicators from Lemma 1. However, the exact representation is analytically complex and harder to evaluate compared to the normal representation of performance indicators we derive in this paper.

Appendix C Application of Lemma 1

Lemma 1 holds regardless of the structure of the left sub-chain (sub-chain 1). For example, if the right sub-chain (sub-chain 2) is a single state s , then using the relationships $\pi_s^1 = P_{block}$ (by definition) and $\pi_s^2 = 1$, we obtain an (obvious) general representation for the “Erlang B” model (where the left sub-chain is not necessarily an M/M/s/s queue): $P_Q = P_{ab} = P_{block}$. Another example is that if the right sub-chain is an M/M/1 queue with system utilization $\rho \doteq \lambda/(s\mu)$, then using the relationships $\pi_s^1 = P_{block}$ (by definition), $\pi_s^2 = 1 - \rho$, $p = -a$, and $a = (s - R)/R = (1 - \rho)/\rho$, we obtain a general representation for the “Erlang C” model (where again, the left sub-chain is not necessarily an M/M/s/s queue): $P_Q = \frac{P_{block}}{1 - \rho + \rho P_{block}}$ and $P_{ab} = 0$. These relationships can be confirmed for the standard Erlang C model by a direct calculation (for example, see Equation (15.5) in [3]).

Lemma 1 and Corollary 3 are both exact, and therefore can be utilized when deriving non-asymptotic formulae for performance indicators, but can also be utilized to obtain approximate results. For example, if π_s is small, π_s can be dropped from Equations (9), (10), and (11) to obtain the following approximate expressions:

$$\begin{aligned} P_Q &\approx P_{Q-}, \\ P_{ab} &\approx pP_{Q-}, \\ L_Q &\approx \frac{\lambda}{\theta} \cdot (p - \varepsilon)P_{Q-} = \frac{\lambda_Q - s\mu_Q}{\theta}P_{Q-}. \end{aligned}$$

These approximate expressions are useful when staffing level s is either in shortage or in excess enough to make π_s close to 0. For example, if s is in extreme shortage, π_s^2 gets close to 0 while π_s^1 does not, and therefore, we can approximate π_s by 0 and P_{Q-} by 1, in which case the above approximate expressions become a frequently used heavy-traffic approximation: $P_Q \approx 1$, $P_{ab} \approx p$, and $L_Q \approx \frac{\lambda_Q - s\mu_Q}{\theta}$.

Appendix D Comparison of Non-Asymptotic Representation and Square-root Staffing Rule for Erlang A model

For simplicity, define $\phi(c)$ and $\omega(c)$ as follows (note: $\phi(c)$ is defined in Equation (22)):

$$\phi(c) \doteq \frac{\frac{\sqrt{\mu_Q/\theta}}{h(\sqrt{\mu_Q/\theta \cdot c})}}{\frac{1}{h(-c)} + \frac{\sqrt{\mu_Q/\theta}}{h(\sqrt{\mu_Q/\theta \cdot c})}} \text{ and } \omega(c) \doteq \frac{1}{\frac{1}{h(-c)} + \frac{\sqrt{\mu_Q/\theta}}{h(\sqrt{\mu_Q/\theta \cdot c})}}.$$

Specifically, for the original Erlang A reneging model, we assume $\mu_Q = \mu$ and $\theta = \gamma$, and denote

$$\phi^A(c) \doteq \frac{\frac{\sqrt{\mu/\gamma}}{h(\sqrt{\mu/\gamma \cdot c})}}{\frac{1}{h(-c)} + \frac{\sqrt{\mu/\gamma}}{h(\sqrt{\mu/\gamma \cdot c})}} \text{ and } \omega^A(c) \doteq \frac{1}{\frac{1}{h(-c)} + \frac{\sqrt{\mu/\gamma}}{h(\sqrt{\mu/\gamma \cdot c})}}.$$

Denote also that $p^A \doteq -c/\sqrt{R}$, which is Equation (7) for the $\mu_Q = \mu$ case. Then the square-root staffing rule for the original Erlang A reneging model is represented as follows:

$$P_Q = \phi^A(c) \text{ and } P_{ab} = \frac{\omega^A(c)}{\sqrt{R}} + p^A \cdot \phi^A(c). \quad (23)$$

In contrast, by assuming $\varepsilon = \tau = 0$ in Tables 4 and 5, a non-asymptotic representation of P_{Q-} and π_s becomes

$$P_{Q-}^A \doteq \frac{\frac{\sqrt{\mu/\gamma}}{h(\sqrt{\mu/\gamma} \cdot c + \Delta')}}{\frac{1}{h(-c-\Delta)} + \frac{\sqrt{\mu/\gamma}}{h(\sqrt{\mu/\gamma} \cdot c + \Delta')}} \text{ and } \pi_s^A \doteq \frac{\frac{1}{\sqrt{R}}}{\frac{1}{h(-c-\Delta)} + \frac{\sqrt{\mu/\gamma}}{h(\sqrt{\mu/\gamma} \cdot c + \Delta')}}.$$

Then using Corollary 3, our non-asymptotic formulae for the original Erlang A reneging model become

$$P_Q = \pi_s^A + P_{Q-}^A \text{ and } P_{ab} = \pi_s^A + p^A \cdot P_{Q-}^A, \quad (24)$$

By comparing Equations (23) and (24), we can see that the term corresponding to π_s^A is missing from P_Q of the square-root staffing rule. Note that the continuity correction terms (Δ and Δ') are also missing in the square-root staffing rule, but their contributions are smaller than π_s^A .

Remark D.1. *Using our non-asymptotic representation, we can derive a more general square-root staffing rule for the modified Erlang A reneging model with $R = R_Q$ (i.e., $\varepsilon + \tau = 0$). By assuming $\varepsilon + \tau = 0$ in Tables 4 and 5 and ignoring all continuity correction terms, a non-asymptotic representation of P_{Q-} and π_s becomes*

$$P_{Q-} = \phi(c) \text{ and } \pi_s = \frac{\omega(c)}{\sqrt{R}}.$$

Denote that $p^ \doteq \varepsilon - (1 - \varepsilon)c/\sqrt{R}$, which is Equation (7) for the $\varepsilon + \tau = 0$ case. Then using Corollary 3, the square-root staffing rule for the modified Erlang A reneging model with $R = R_Q$ is represented as follows:*

$$P_Q = \phi(c) + \frac{\omega(c)}{\sqrt{R}} \text{ and } P_{ab} = \frac{\omega(c)}{\sqrt{R}} + p^* \cdot \phi(c). \quad (25)$$

Equation (25) is more general and precise (for P_Q) than Equation (23) (the original square-root staffing rule) but is not as accurate as our non-asymptotic representation because of missing the continuity correction terms.

References

- [1] F. P. Kelly, Reversibility and Stochastic Networks, John Wiley & Sons, 1979.
- [2] L. Kleinrock, Queueing Systems, Volume I: Theory, John Wiley & Sons, 1975.
- [3] M. Harchol-Balter, Performance Modeling and Design of Computer Systems: Queueing Theory in Action, Cambridge University Press, 2013
- [4] E. G. Coffman Jr, A. A. Puhalskii, M. I. Reiman, P. E. Wright, Processor-shared buffers with reneging, Performance Evaluation 19 (1) (1994) 25–46.